The Astrophysical Journal, 713:212–219, 2010 April 10 doi:10.1088/0004-637X/713/1/212


# EXTINCT $^{93}$Zr IN SINGLE PRESOLAR SiC GRAINS FROM LOW MASS ASYMPTOTIC GIANT BRANCH STARS AND CONDENSATION FROM Zr-DEPLETED GAS

Y. Kashiv[1,6], A. M. Davis[1], R. Gallino[2], Z. Cai[3], B. Lai[3], S. R. Sutton[4], and R. N. Clayton[5]
[1] Department of the Geophysical Sciences and Enrico Fermi Institute, University of Chicago, Chicago, IL 60637, USA; yoavk@phys.huji.ac.il
[2] Dipartimento di Fisica Generale, Università di Torino, Via P. Giuria 1, I-10125 Torino, Italy
[3] Advanced Photon Source, Argonne National Laboratory, Argonne, IL 60439, USA
[4] Consortium for Advanced Radiation Sources and Department of the Geophysical Sciences, University of Chicago, Chicago, IL 60637, USA
[5] Departments of Chemistry and the Geophysical Sciences and Enrico Fermi Institute, University of Chicago, Chicago, IL 60637, USA
*Received 2009 October 6; accepted 2010 February 13; published 2010 March 19*

## ABSTRACT

Synchrotron X-ray fluorescence was used in this study for the first time to measure trace element abundances in single presolar grains. The abundances of Zr and Nb were determined in SiC grains of the KJF size-separate. These grains are most likely from C-rich asymptotic giant branch stars (mainstream grains). Comparison of the data with *s*-process calculations suggests that the relatively short-lived isotope $^{93}$Zr ($t_{1/2} = 1.5 \times 10^6$ yr) condensed into the grains. The Nb/Zr ratios of the majority of the grains are higher than the *s*-process and CI chondrite ratios. This is probably due to grains condensing from stellar gas that was depleted in Zr, potentially because of earlier condensation of ZrC, but not depleted in Nb. However, grain contamination with solar system Nb is possible as well. Upper limits on the initial $^{93}$Zr/Zr ratios in the grains agree with the ratios observed in late-type S stars.

*Key words:* astrochemistry – circumstellar matter – nuclear reactions, nucleosynthesis, abundances – stars: abundances – stars: AGB and post-AGB

*Online-only material:* color figures

## 1. INTRODUCTION

Presolar grains are stardust grains that condensed in outflows of stars that lived before the formation of the solar system. The source stars of presolar grains are among the stars that contributed material to the Solar Nebula. The grains survived the formation of the solar system and are found today mainly in primitive meteorites (Anders & Zinner 1993; Zinner 1998; Clayton & Nittler 2004). In addition, presolar grains were found as well in interplanetary dust particles (IDPs; Messenger et al. 2003), Antarctic micrometeorites (Yada et al. 2005), dust from Comet Wild 2 that was collected by the Stardust mission (McKeegan et al. 2006) and IDPs associated with Comet Grigg-Skjellerup (Nguyen et al. 2007). As a consequence of their circumstellar origin, the elemental and isotopic compositions of the grains provide a wealth of information on the composition of the source stars, on nuclear reactions operating within them and on grain condensation in stellar winds.

Due to very large isotopic anomalies of nucleosynthetic origin in them, all SiC grains in primitive meteorites are identified as presolar. They are classified on the basis of the isotopic compositions of Si, C, and N (Hoppe et al. 1994). The most abundant class of SiC grains, called mainstream grains (Zinner 1998), makes up 93% of all SiC grains (Nittler & Alexander 2003). The source stars of mainstream SiC grains are thought to be low-mass (1.2–4 $M_\odot$) C-rich asymptotic giant branch (AGB) stars. Stellar models (Gallino et al. 1998) and observations (Smith & Lambert 1990) point to these stars as the site where the main component of the *s*-process operates. This association is further supported by *s*-process signature in the isotopic compositions of heavy elements in the grains (Lugaro et al. 2003).

Travaglio et al. (2004) combined *s*-process calculations with analysis of observations of elemental abundances as a function of stellar metallicity. They concluded that 67% of the solar inventory of $^{93}$Nb, the only stable isotope of Nb, is produced by the main component of the *s*-process, in low- and intermediate-mass AGB stars, as radioactive $^{93}$Zr ($t_{1/2} = 1.5 \times 10^6$ yr). Due to its short half-life compared to the lifetime of low-mass stars ($\sim 10^9$ yr) and the fact that the AGB phase occurs at the end of the star's life, $^{93}$Zr in stars has to be synthesized locally and could not be inherited from other stars. Observations of $^{93}$Zr in spectra of late type S stars (in the ZrO molecule; Peery & Beebe 1970; Zook 1985; Lambert et al. 1995) support the *s*-process models. On the other hand, the half-life of $^{93}$Zr is long compared with the $\sim 10^6$ yr time of the AGB phase (a few $10^5$ yr from that are the C-rich phase (Gallino et al. 1998), which is required for condensation of SiC grains) and the few years timescale for condensation of a $\sim 1$ $\mu$m SiC grain in the stellar wind (Sharp & Wasserburg 1995). In addition, mainstream SiC grains bear evidence for extinct radioisotopes, some with shorter half-lives than $^{93}$Zr. Large excesses in $^{26}$Mg in many grains indicate that $^{26}$Al ($t_{1/2} = 7.1 \times 10^5$ yr), which is produced in AGB stars as well, though not by the *s*-process, condensed into the grains (Zinner 1998). Savina et al. (2004) found excesses in $^{99}$Ru in 19 grains, which indicate that the *s*-process radioisotope $^{99}$Tc ($t_{1/2} = 2.13 \times 10^5$ yr) condensed into the grains. Depletions in $^{135}$Ba in many grains indicate that its volatile parent, *s*-process produced $^{135}$Cs ($t_{1/2} = 2.3 \times 10^6$ yr), was alive at the time of grain condensation, but did not condense into the grains (Lugaro et al. 2003). All this suggests that $^{93}$Zr was still alive at the time grains condensed in the source AGB stars. Hence, evidence that live $^{93}$Zr condensed into mainstream SiC grains would be complimentary to the data on $^{26}$Al, $^{99}$Tc, and $^{135}$Cs, and will add to the grain association with AGB stars (see Busso et al. 1999 for a discussion of nucleosynthesis

[6] Present address: Department of Physics, University of Notre Dame, Notre Dame, IN 46556, USA and Racah Institute of Physics, Hebrew University of Jerusalem, Jerusalem 91904, Israel.

in AGB stars). However, unlike with $^{26}$Al, $^{99}$Tc, and $^{135}$Cs, where the evidence is based on the abundances of the daughter isotopes, $^{26}$Mg, $^{99}$Ru, and $^{135}$Ba, in the case of $^{93}$Zr, the evidence needs to be based on the Nb elemental abundance, since it is monoisotopic.

## 2. EXPERIMENTAL

The technique of synchrotron X-ray fluorescence (SXRF) was applied to the analysis of trace elements in presolar grains for the first time in this study (preliminary results were presented in Kashiv et al. 2001, 2002, 2006). The experiments were done at the Advanced Photon Source (APS) at the Argonne National Laboratory: measurements were done at X-ray Operations and Research (beamline 2-ID-D) and data analyses at GeoSoilEnviroCARS (sector 13).

Forty-one single presolar SiC grains from the Murchison (CM2) meteorite KJF size-separate (mass-weighted median size of 1.86 $\mu$m; Amari et al. 1994) were analyzed in three runs, each grain with a different primary X-ray beam energy: 18.0, 22.5, and 24.5 keV. The size of the beam focal point was about 0.6 $\mu$m × 0.6 $\mu$m, i.e., smaller than the grain size. The grains were deposited on a 7 $\mu$m thick Kapton film. The low atomic number, low density, and mechanically strong Kapton plastic ($C_{22}H_{10}N_2O_5$, $\rho = 1.43$ g cm$^{-3}$) was chosen in order to minimize scattering of primary X-rays from the substrate. Due to the small size of the grains compared to the substrate thickness, scattering off the substrate was the main source of background. This background appeared in the spectra as the low energy tail of the Compton scattering peak. The tail was flat for the most part and spanned the full spectrum under the elemental fluorescence peaks.

"Raw" spectra were collected for the grains with acquisition times ranging from 10 to 45 minutes. The abundances of both Zr and Nb were determined in 19 of the grains. Zirconium abundances were measured in 19 additional grains, while only upper limits were determined in the remaining three grains. The primary beam energy was too low to detect Nb in the seven grains measured at 18.0 keV, and only upper limits were determined in the remaining 15 grains. Due to time limitations, individual background spectra with the same acquisition times were collected for 19 of the 41 grains. They were taken on the Kapton substrate a few $\mu$m away from each grain, in order to account for potential spatial inhomogeneities in the substrate. The background spectra at each primary beam energy turned out to be almost identical. Utilizing this observation, general background spectra were generated for each primary beam energy, by summing the individual background spectra, and used for the grains without individual background spectra.

The intensity of the Compton peak in the background spectrum of each grain was normalized to that of the Compton peak in the grain's "raw" spectrum (the intensities of the Compton peaks in the "raw" and background spectra were similar for grains with individual background spectra, due to the fact that in both cases scattering was primarily from the substrate). The background spectrum was then multiplied by the normalizing factor and subtracted from the "raw" grain spectrum to generate a "reduced" grain spectrum. The validity and efficiency of this process was exhibited by the observation that the background in the "reduced" grain spectra was very low. Elemental fluorescence peaks (K$\alpha$, K$\beta$, etc.) and the background were fitted in the "reduced" grain spectra and the little leftover background

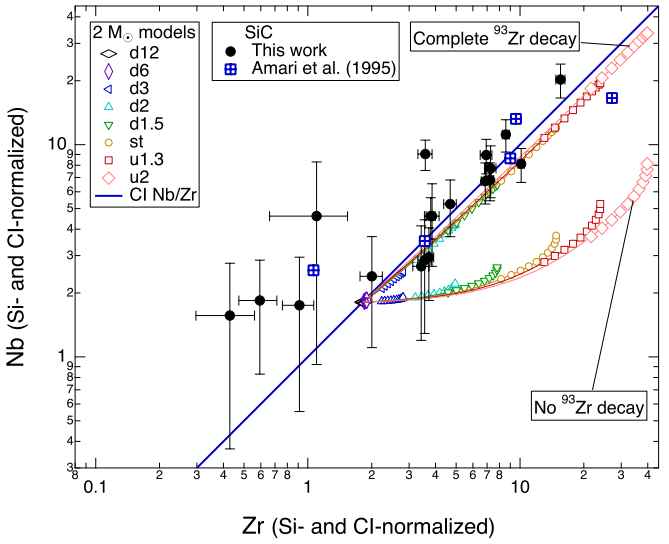


**Figure 1.** Comparison between presolar SiC grain data and *s*-process calculations for a 2 $M_\odot$ AGB star of solar metallicity. Values are enrichment factors, normalized using the new CI chondrite Zr and Nb abundances of Lodders et al. (2009). Uncertainties (statistical) are $2\sigma$. Upper limits are not plotted, but are given in Table 1. (Their omission does not affect the conclusions and it adds to the clarity of the figure). The grains of this study are of the KJF size-separate. The results of Amari et al. (1995) are for mainstream SiC grains of the KJH size-separate (uncertainties were not reported for individual data points). The diagonal solid blue line is the CI chondrite Nb/Zr ratio of Lodders et al. (2009). d12, d6, d3, d2, d1.5, st, u1.3, and u2 are models with $^{13}$C pocket intensities ranging from 1/12× to 2× the standard case (st, see the text; Lugaro et al. 2003). Note that the same symbols are used for both the "Complete $^{93}$Zr decay" and "No $^{93}$Zr decay" arrays.

(A color version of this figure is available in the online journal.)

was subtracted from the peaks. Trace element abundances were determined by normalizing the intensities of their K$\alpha$ peaks in the "reduced" grain spectra to the intensity of the Si K$\alpha$ peak, and setting the Si abundance to its concentration in SiC, 70% by mass (50% by atom). The following corrections were applied to the trace-element/Si K$\alpha$ peak intensity ratios: (1) the dependence of the ionization cross sections on the primary X-ray beam energy, (2) X-ray line transition probabilities and fluorescence yields, (3) the dependence of fluorescence self-absorption by the grains and by the detector filters on X-ray line energy, (4) grain size and detector filter thickness, (5) grain and filter compositions, and (6) the energy dependence of the detector response. Note that since trace element abundances were determined by normalizing their K$\alpha$ peaks to that of Si, the abundances do not necessarily correlate with the signal-to-noise ratio (as is evident from the fact that the uncertainties in Figure 1 do not necessarily correlate with the Zr and Nb abundances). The reason for this is that although the background (primarily from the Kapton substrate) was similar for every grain, the intensity of the Si K$\alpha$ peak varied from grain to grain. However, by normalizing the trace element peak intensities to that of Si, experimental systematic effects were eliminated and trace element abundances could be determined. More experimental detail and abundances of other trace elements can be found in Kashiv (2004) and will be published elsewhere.

The C, N, and Si isotopic compositions of the grains were not measured, so the grains could not be individually classified. However, due to the overwhelming abundance of mainstream grains among presolar SiC grains, the reasonable assumption that the grains are mainstream was made and used in interpreting the data.

## 3. RESULTS AND DISCUSSION

### 3.1. The Correlation between Nb and Zr

The Zr and Nb abundances, expressed as enrichment factors (enrichment factor = $(te/Si)_{SiC}/(te/Si)_{CI}$, where te = the Zr, Nb abundance and CI = the CI chondrite abundance), are given in Table 1 and are plotted in Figure 1. The secondary ion mass spectrometry (SIMS) results of Amari et al. (1995) for individual mainstream grains of the KJH size-separate (mass-weighted median size of 4.57 $\mu$m; Amari et al. 1994) are plotted as well. For clarity, upper limits are not plotted for either data set, but their omission does not affect the conclusions. Amari et al. (1995) measured as well aggregates of grains of the smaller size-separates KJA through KJF. However, the data for the KJF aggregate (the size-separate measured by us) are not presented here. The reason is that the aggregate appeared to have been contaminated with zircon grains, which resulted in very high Zr abundance.

The new CI chondrite Zr and Nb abundances of Lodders et al. (2009) were used to calculate the enrichment factors of the two data sets. The new values are Zr = 10.4 and Nb = 0.788, in units of atoms per $10^6$ atoms of Si. In addition to the experimental data, results of calculations of the abundances of these two elements in the envelope of a 2 $M_\odot$ AGB star of initially solar composition are plotted as well. Apart from the new CI chondrite abundances of Zr and Nb, these calculations use the same cross sections and isotopic abundances as were used earlier and are done for eight $^{13}$C pocket intensities, d12, d6, d3, d2, d1.5, st, u1.3, and u2 (Lugaro et al. 2003). The standard case, st, has $^{13}$C amount that best reproduces the elemental abundances of the *s*-process main component in the solar system in a model of an AGB star with half solar metallicity (Gallino et al. 1998). d12,. . ., d1.5 are AGB star models with 1/12,. . ., 1/1.5 the $^{13}$C amount of the st case, and u1.3, u2 are models with $\times$1.3, $\times$2 the $^{13}$C amount of the st case. In plotting the results of the calculations, it was assumed that 100% of Zr and Nb and 56.2% of Si condensed into the grains. These fractions are derived from the calculations of Lodders & Fegley (1995) and the CI chondrite S abundance recommended by Lodders et al. (2009).[7]

Two arrays of results of calculations are plotted in Figure 1. One array, labeled "No $^{93}$Zr decay," represents the expected Nb abundance in the grains without the radiogenic contribution from $^{93}$Zr. The second array, labeled "Complete $^{93}$Zr decay," represents the expected Nb abundance in the grains after $^{93}$Zr has fully decayed.

As can be seen in Figure 1, the two experimental data sets agree with one another, except for one Zr-rich grain in the Amari et al. (1995) data set, and both plot close to the "Complete $^{93}$Zr decay" array. The relatively good agreement between the grain data and the calculated radiogenic array, combined with the relatively short $^{93}$Zr half life, indicates that freshly *s*-process synthesized $^{93}$Zr condensed into the SiC grains as they were forming in the winds from low mass AGB stars, and that most of the Nb in the grains is the product of the *in situ* decay of $^{93}$Zr. If the assumption that the SiC grains are mainstream grains is correct, this result adds to the evidence in the grains for extinct $^{26}$Al, $^{99}$Tc, and $^{135}$Cs. It adds as well to the identification of low mass AGB stars as the source stars of mainstream SiC grains and the site of the *s*-process main component nucleosynthesis.

Another interesting thing to note in Figure 1 is that the Nb/Zr ratio (atom) of the radiogenic *s*-process results array ("Complete $^{93}$Zr decay"), $\approx$ 0.062, is lower than the new CI chondrite ratio, 0.076. (Note that the Zr and Nb abundances are plotted in Figure 1 as enrichment factors, which need to be

**Table 1**
Zr and Nb Abundances in the Single Presolar SiC Grains of this Study[a,b,c]

| Grain | Zr | Nb |
|---|---|---|
| 18-02N | 17.34 ± 0.23 | |
| 18-08N | <0.08 | |
| 18-15Na | 0.57 ± 0.06 | |
| 18-15Nb | 0.97 ± 0.07 | |
| 18-18Na | 2.57 ± 0.10 | |
| 18-18Nb | 3.80 ± 0.14 | |
| 18-25N | 0.19 ± 0.06 | |
| 22.5-1 | 4.7 ± 0.3 | 5.1 ± 1.5 |
| 22.5-2 | 0.93 ± 0.21 | <4 |
| 22.5-3 | 0.55 ± 0.13 | <2.8 |
| 22.5-4 | 1.99 ± 0.24 | 2.3 ± 1.2 |
| 22.5-6 | 3.4 ± 0.3 | 2.6 ± 1.4 |
| 22.5-7 | 0.42 ± 0.14 | 1.5 ± 1.1 |
| 22.5-9 | 2.9 ± 0.4 | <4 |
| 22.5-10 | 0.60 ± 0.19 | <2.6 |
| 22.5-12 | 0.74 ± 0.24 | <6 |
| 22.5-14 | 6.9 ± 0.4 | 8.6 ± 1.6 |
| 22.5-16 | 4.2 ± 1.5 | <34 |
| 22.5-17 | 3.57 ± 0.28 | 8.7 ± 1.4 |
| 22.5-19 | 1.73 ± 0.21 | <3 |
| 22.5-21 | 0.29 ± 0.13 | <2.7 |
| 22.5-22 | 15.5 ± 0.8 | 20 ± 3 |
| 24.5-02 | 5.3 ± 0.7 | <8 |
| 24.5-04a | 3.5 ± 2.6 | <26 |
| 24.5-08 | 7.20 ± 0.28 | 6.6 ± 1.3 |
| 24.5-14a | 3.8 ± 0.3 | 4.4 ± 1.9 |
| 24.5-15 | 7.2 ± 0.4 | 7.5 ± 2.0 |
| 24.5-16a | 3.54 ± 0.25 | 2.8 ± 1.5 |
| 24.5-16b | 3.70 ± 0.19 | 2.8 ± 1.1 |
| 24.5-17 | 0.59 ± 0.12 | 1.8 ± 1.0 |
| 24.5-18 | 1.4 ± 0.3 | <4 |
| 24.5-20 | 3.79 ± 0.19 | 4.5 ± 1.0 |
| 24.5-21 | 1.02 ± 0.14 | <2.6 |
| 24.5-21a | 2.0 ± 0.4 | <8 |
| 24.5-25 | <0.5 | <2.9 |
| 24.5-30 | 0.91 ± 0.16 | 1.7 ± 1.2 |
| 24.5-32a | 8.6 ± 0.4 | 10.7 ± 1.8 |
| 24.5-33 | 6.8 ± 0.3 | 6.4 ± 1.4 |
| 24.5-35a | <0.3 | <1.6 |
| 24.5-36a | 10.1 ± 0.3 | 7.8 ± 1.4 |
| 24.5-36b | 1.1 ± 0.4 | 4 ± 3 |

**Notes.** Values presented as enrichment factors. The new CI chondrite Zr and Nb values of Lodders et al. (2009) were used for normalization. Uncertainties (statistical) are 2$\sigma$. The number at the beginning of each grain's name indicates the primary X-ray beam energy at which it was measured. The 18.0 keV primary beam energy was too low to measure Nb.

[a] Enrichment factor = $(te/Si)_{SiC}/(te/Si)_{CI}$, where te is the Zr, Nb abundance and CI is the CI chondrite abundance.

[b] Upper limits are given when the 2$\sigma$ uncertainty exceeds the enrichment factor, or when a peak is not seen in the spectrum, and are given as the enrichment factor plus the 2$\sigma$ uncertainty.

[c] To convert abundance to ppmw, multiply the Zr enrichment factor by 23.65 and that of Nb by 1.83. To convert to ppma, multiply the Zr enrichment factor by 5.19 and that of Nb by 0.39.

[7] Lodders & Fegley (1995) calculated, using the Anders & Grevesse (1989) solar abundances, that 50% of the Si in the envelopes of C-rich AGB stars condenses into crystalline SiC, while the other 50% of Si is bound as gas-phase SiS. Using the CI chondrite S abundance recommended by Lodders et al. (2009; $4.38 \times 10^5$ in units of atoms per $10^6$ atoms of Si), the value above is adjusted to 56.2% of Si condensing into SiC.

converted according to footnote c in Table 1 in order to get the elemental ratio). This is due to the fact that the new CI chondrite abundances were used to derive the Zr and Nb enrichment factors. As mentioned above, the new CI chondrite abundances of the two elements were used in the *s*-process calculations presented here. However, the new abundances did not affect the results. This is because the resulting abundances are determined primarily by the neutron capture cross sections and only depend weakly on the starting composition. The discrepancy between the CI chondrite and *s*-process Nb/Zr ratios suggests that the ratio in massive stars is higher than the CI chondrite ratio. Mixing of the higher than CI chondrite Nb/Zr ratio in massive stars with the lower than CI chondrite ratio of the *s*-process main component resulted in the CI chondrite ratio. This observation is further supported by the Travaglio et al. (2004) conclusion that $\approx$ 35% of the solar abundance of both Zr and Nb came from massive stars.

### 3.2. Zirconium Depletion

As noted in Section 3.1, the experimental data points of this study plot close to the "Complete $^{93}$Zr decay" array in Figure 1. However, the majority of grains (15 of 19 grains) plot to the left of the array, meaning that the grains are depleted in Zr or enriched in Nb relative to the radiogenic array. Furthermore, 17 of the 41 grains measured (Table 1) have Zr enrichment factors that are more than $2\sigma$ lower than 1.78 (= 100%/56.2%), the calculated minimum Zr enrichment factor (Section 3.1). The 17 grains include four for which both Zr and Nb were measured (22.5-7, 24.5-17, 24.5-30, 24.5-36b, all plotted), seven for which Zr was measured but only Nb upper limits were determined (22.5-2, 22.5-3, 22.5-10, 22.5-12, 22.5-21, 24.5-18, 24.5-21), three for which only Zr was measured (18-15Na, 18-15Nb, 18-25N), two for which only Zr and Nb upper limits were determined (24.5-25, 24.5-35a) and one for which only Zr upper limit was determined (18-08N). Ten of the 17 grains have Zr enrichment factors that are even more than $2\sigma$ lower than 1, the assumed initial CI chondrite composition of the AGB stars. Such low enrichment factors are very difficult to explain by single star nucleosynthesis or galactic chemical evolution. In the *s*-process, the Zr/Si can only increase from the assumed initial CI chondrite composition. The most likely explanation for the displacement and spread of the data points, including the extreme ones, is condensation of the SiC grains from Zr-depleted stellar gas.

Depletion of Zr is expected from equilibrium thermodynamic calculations of condensation and has experimental support. Zirconium is calculated to be one of the first elements to condense, as ZrC, under C/O >1 conditions (Lodders & Fegley 1995). Once ZrC condensed, it could have been removed from equilibrium with the gas before SiC condensation, hence depleting the gas in Zr. One mechanism for removing ZrC from the gas could have been by being enclosed in the two much more abundant grain phases TiC and graphite, or by reacting with the gas to form a ZrC–TiC solid solution. Taking into account the Zr enrichment in the gas due to the *s*-process, both TiC and graphite have condensation temperatures ($T_{\rm cond}$) ~200 K lower than the $T_{\rm cond}$ of ZrC and ~150 K higher than the $T_{\rm cond}$ of SiC (Lodders & Fegley 1995). Indeed, subgrains of the carbide solid solution $(Ti_{1-(x+y+z)}Zr_xMo_yRu_z)C$, ranging in composition from nearly TiC to nearly (Zr,Mo)C, were detected in graphite grains from C-rich AGB stars (Bernatowicz et al. 1996; Croat et al. 2005). The Zr/Mo ratio of the subgrains ranged from early condensing, Zr enriched, to later condensing, Zr depleted (MoC is less refractory than ZrC). The subgrains served as heterogeneous condensation nuclei for the graphite grains (subgrains found in the center of graphite grains) or were captured later as the graphite grains were growing (subgrains found off center of graphite grains). Another possible mechanism for Zr depletion is that early condensing ZrC grains were blown away by radiation pressure and decoupled from the parcel of gas in which they condensed (Lodders & Fegley 1997). Then, by the time SiC condensed in the same parcel of gas, ZrC grains were not present and hence the gas was depleted in Zr. This mechanism was invoked to explain enrichment of the less refractory Mo relative to Zr in some of the carbide subgrains mentioned above (Bernatowicz et al. 1996; T. J. Bernatowicz 2006, private communication).

Indirect support for Zr depletion comes as well from the Ti/Si ratio in the grains of this study (Kashiv 2004, will be published separately). Both Si and Ti are not affected for the most part by the *s*-process. Hence, their abundances in the source AGB stars of the grains are expected to be CI chondrite, as the assumed initial composition of the stars. As mentioned above, TiC, like ZrC, is more refractory than SiC. Since 56.2% of Si is calculated to condense into SiC (Section 3.1), the minimum possible Ti enrichment factor in the grains without Ti depletion in the gas, as with Zr, is 1.78 (higher values are expected for early condensing SiC grains). However, the Ti enrichment factors in most grains are lower than 1.78 and in many cases are even lower than 1, the assumed initial CI chondrite composition of the AGB stars. Similar values were measured by Amari et al. (1995). This clearly indicates depletion of Ti, which is less refractory than Zr.

The problem with these scenarios is that Nb, like Zr, is a very refractory element as well. Taking into account the fact that according to the calculations, at the time of grain condensation the atomic Nb/Zr ratio in the AGB star envelope could have been as low as 0.0125 (a factor $\approx$ 6 lower than the new CI chondrite ratio, 0.076, since most of the Nb in AGB stars is produced as $^{93}$Zr; Figure 1), equilibrium thermodynamics predict that NbC will condense at a temperature that is ~40 K lower than the $T_{\rm cond}$ of ZrC and ~150 K higher than the $T_{\rm cond}$ of TiC and graphite (Lodders & Fegley 1995). This means that NbC, like ZrC, is expected to have condensed and been removed from the stellar gas by TiC and graphite, and/or by radiation pressure. In case this did not happen, as is suggested by our model, a possible explanation is that the kinetics of growth of NbC grains, and/or the addition of Nb atoms to trace element carbide solid solution (ZrC, TiC), was not fast enough. Bernatowicz et al. (2005) showed that the kinetics of growth of graphite, TiC and ZrC grains in spherically symmetric outflows from C-rich AGB stars is too slow to allow growth to the grain sizes measured in the laboratory (Bernatowicz et al. 1996; Croat et al. 2005), and hence the grains must have condensed in anisotropic outflows. In the case of Nb, it may be that due to its low abundance in the envelopes of these stars, down to 0.0125 of the Zr abundance, significant condensation of NbC was too slow and as a consequence Nb was not depleted in the gas. However, when SiC condensed, due to its much higher abundance than earlier condensing trace element carbides, the low Nb abundance was less limiting and Nb could have condensed into SiC in solid solution.

Niobium was not detected to date in the carbide solid solution subgrains in graphite grains from C-rich AGB stars (Bernatowicz et al. 1996; Croat et al. 2005). While this could have been an additional experimental evidence for our model, it appears that the reason, at least in part, for no detection

was that the expected Nb abundances in the subgrains were below the detection limit of the experimental method used in these studies, transmission electron microscopy (TEM). The Nb/Zr detection limit of the TEM under the conditions used by Bernatowicz et al. (1996) and Croat et al. (2005) was 0.06–0.21, with an average of 0.13 ± 0.06 (T. K. Croat 2007, private communication). The calculated *s*-process fraction of $^{93}$Zr is up to 0.05 of Zr (Figure 3). This means that if the carbide subgrains contained only radiogenic Nb from the decay of $^{93}$Zr, which is definitely present in the subgrains (due to the presence of Zr), it could not have been detected. On the other hand, if the subgrains contained in addition nonradiogenic Nb as well, and in similar abundances to the nonradiogenic Nb in the SiC grains, it would have resulted in Nb/Zr >0.05. In this case it is not clear whether the Nb abundances were high enough to have been detected. Sixteen of the 19 SiC grains with both Zr and Nb detections have 0.06 < Nb/Zr <0.19, which is in the range of the TEM detection limit. The remaining three SiC grains have 0.23 < Nb/Zr <0.31, i.e., above the TEM detection limit. In summary, it is unclear whether the lack of Nb detection in the carbide subgrains was due to the low abundances of radiogenic Nb only, which would support our model, or due to higher Nb abundances (including nonradiogenic Nb) that were still below the TEM detection limit, which would weaken our model.

Zirconium depletion from the gas, without Nb depletion, produces curved arrays that are displaced to the left of the "Complete $^{93}$Zr decay" array in Figure 1 to an extent that is proportional to the degree of depletion. Thus, condensation of SiC grains from stellar gas with varying degrees of Zr depletion, corresponding to different stars and/or different stages in the AGB phase of the same star(s), generates the observed spread in the grains' Nb/Zr ratios. The measured grain data could be explained by applying this scenario to AGB stars in the mass range of ∼1.5–3 $M_{\odot}$, which agrees with the inferred mass range of the grains' source stars based on the isotopic composition of heavy trace elements in the grains (Lugaro et al. 2003). An example of this scenario is shown in Figure 2 for a 2 $M_{\odot}$ AGB star. In this example, hypothetical "Complete $^{93}$Zr decay" arrays are plotted for cases where 50%, 80%, 90%, and 95% of Zr was lost from the gas by the time SiC started to condense (the 0% Zr-loss array is identical to the "Complete $^{93}$Zr decay" array in Figure 1). As can be seen, the measured compositions of all the grains of this study and of Amari et al. (1995) could be explained by these arrays.

### 3.2.1. Possible Nb Contamination

Another possibility that needs to be considered is that the high Nb/Zr ratios in the grains are due to contamination with solar system Nb (in the Murchison meteorite[8] and/or in the laboratory). Two studies in recent years give indirect support to this possibility. In the first, Barzyk et al. (2006) used resonance ionization mass spectrometry (RIMS) to measure the isotopic composition of Zr, Mo, and Ba in single SiC grains of the Murchison KJH size-separate. They showed that Zr is less contaminated than Mo and Ba in the grains, or potentially not contaminated at all. This suggests that if the grains studied

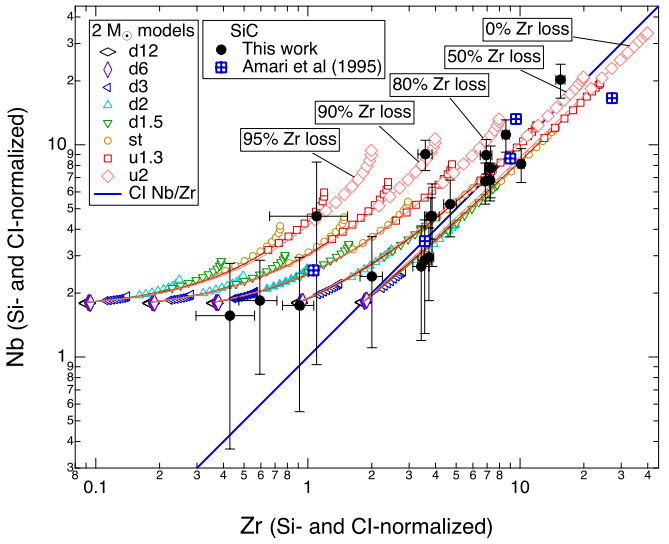


**Figure 2.** "Complete $^{93}$Zr decay" arrays for SiC grains condensing from gas of a 2 $M_{\odot}$ AGB star with varying degrees of Zr depletion (see the text). The array labeled "0% Zr loss" is identical to the "Complete $^{93}$Zr decay" array in Figure 1. Data and nucleosynthetic calculations are the same as in Figure 1.
(A color version of this figure is available in the online journal.)

by us are contaminated, it is more likely to affect Nb. In the second study, Knight et al. (2008) used SXRF to analyze trace elements in single presolar SiC grains of the Murchison KJG size-separate (mass-weighted median size of 3.02 $\mu$m; Amari et al. 1994). They compared trace element abundances in regular grains with those in grains that were further treated chemically to remove potential contamination from them. The results showed that the presence of some trace elements is due, at least in part, to contamination. While the authors did not report in the preliminary results contamination of Zr or Nb, the results indicate that it is feasible.

As mentioned above, 17 grains have Zr enrichment factors that are more than 2$\sigma$ lower than 1.78 (Table 1), i.e., lower than the calculated minimum enrichment factor (and 10 grains have Zr enrichment factors that are more than 2$\sigma$ lower than 1, the assumed initial CI chondrite composition of the source AGB stars). In order to account for such low Zr abundances, Zr would still need to be depleted in the stellar gas from which the grains condensed. But if the high Nb abundances are due to contamination, the stellar, uncontaminated, Nb abundances in the grains are expected not to be decoupled from Zr. This means that the Zr-undepleted grains would plot on the "0% Zr loss" array in Figure 2 and Nb would be depleted as well in the Zr-depleted grains. The Zr- and Nb-depleted grains would then plot as a continuation of the "0% Zr loss" array at enrichment factors <1.78.

If the grains of this study are indeed contaminated with Nb, it could weaken the proposed mechanism by Barzyk et al. (2006) for the Mo and Ba, but not Zr, contamination of SiC grains. The authors suggested that aqueous activity on the Murchison meteorite parent body could have been responsible for the contamination. That was based on the fact that Mo and Ba are more soluble in seawater than Zr (Bruland & Lohan 2003), and presumably in meteoritic water as well. However, while the Nb solubility in seawater is not known, its upper limit indicates that it is comparable to or lower than that of Zr. In case the grains are contaminated with Nb and by the same process that contaminated them with Mo and Ba, it means

[8] The results of measurements of the Murchison whole rock Nb/Zr ratio (atom), 0.062 (Jochum et al. 2000), 0.084 (Weyer et al. 2002), and 0.070 (Münker et al. 2003), are not high enough to account for the high Nb/Zr ratios measured in this study, up to 0.283, or even for mainstream grains in Amari et al. (1995), up to 0.094. However, there could be as of yet unidentified phase(s) in Murchison with higher Nb/Zr ratio(s) that could be the source of potential contamination.

that either the elemental solubilities in seawater are not a good approximation to those in meteoritic water, or that there was a different contamination mechanism. Another possibility is that the mechanism suggested by Barzyk et al. (2006) is correct for Mo and Ba, but the potential Nb contamination was caused by a separate mechanism.

### 3.2.2. The Possibility of Other SiC Grain Types

As explained above, the isotopic compositions of the grains of this study were not measured and so the grains could not be classified. However, since mainstream grains make up 93% of presolar SiC grains (Nittler & Alexander 2003), our interpretation of the data is based on the assumption that all grains examined here are mainstream SiC. We would like now to consider briefly the possibility that some of the grains belong to the other classes of presolar SiC grains: A, B, X, Y, Z and nova grains.

With respect to the expected Nb/Zr ratio in the grains, the classes above can be divided into two groups. The first group includes grains of types A, B, Y, Z and nova. The second group includes grains of type X. The grains of the types in the first group make up 5.8% of all presolar SiC grains, while X grains make up the remaining 1.2% (Nittler & Alexander 2003).

First group: it is unclear where grains of types A and B originated, and they probably have multiple sources (Amari et al. 2001b; Barzyk et al. 2008), including AGB stars. Grains of types Y and Z are believed to have originated in low metallicity AGB stars (Hoppe et al. 1997; Zinner et al. 2006; Barzyk et al. 2008). The rare nova grains (Amari et al. 2001a) are expected to have compositions between solar and the *s*-process. As a consequence, the Nb/Zr ratios of grains of the first group are not expected to be significantly different from those in mainstream grains. If such grains were among the grains we examined, the data would not allow us to distinguish them from mainstream grains. However, since the grains of this group make up only 5.8% of SiC grains, the probability of them accounting for more than 1–2 grains is very low.

Second group: silicon carbide X grains are thought to have condensed in supernovae (SNe) ejecta (Zinner 1998). However, there are still uncertainties regarding the nucleosynthetic processes that affected the isotopic compositions of heavy trace elements in these grains. In qualitative terms, the discrepancy discussed in Section 3.1, between the new CI chondrite Nb/Zr ratio and the *s*-process ratio (Figure 1), suggests that the Nb/Zr ratio in SN ejecta is higher than the new CI chondrite ratio. Hence, the Nb/Zr ratios in SiC X grains could potentially be high enough to account for the compositions of the 15 of 19 grains with high Nb/Zr ratios. If the 15 grains were SiC X grains, there would be no need to invoke a Zr–Nb fractionation during condensation to explain the high Nb/Zr ratios in these grains. However, since X grains make up only 1.2% of SiC grains, the probability that even one grain of the 19 is an X grain is low and hence X grains could not account for the 15 grains with high Nb/Zr ratios.

### 3.3. Comparison with Astronomical Observations

The results of this study are compared in Figure 3 with the astronomical observations of Zook (1985) and Lambert et al. (1995) of the $^{93}$Zr/Zr fraction in the envelopes of late-type S stars (Peery & Beebe 1970 measured one star, R Cygni, that was one of the two stars measured by Zook 1985, and both studies arrived at the same result, $^{93}$Zr/Zr = 0.05). Detection of Tc in the spectra of some of these stars identifies them as

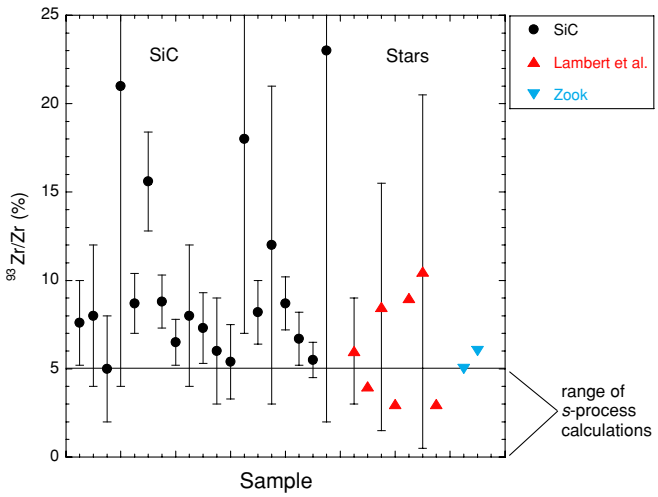


**Figure 3.** Comparison of the Nb/(Zr+Nb) ratios in the SiC grains of this study, which are upper limits on the grains' initial $^{93}$Zr/Zr ratios, and the $^{93}$Zr/Zr ratios in nine late-type S stars. The range of *s*-process results for a 2 $M_{\odot}$ AGB star (without $^{93}$Zr decay) is indicated at the bottom of the plot. Plotted stars are (from left) R And, BI And, T Cam, S Cas, U Cas, AD Cyg, R Gem (Lambert et al. 1995), R Cyg, and V Cnc (Zook 1985). Uncertainties (statistical) are $2\sigma$.
(A color version of this figure is available in the online journal.)

intrinsic AGB stars (i.e., that the *s*-process operates in them). The others are presumed to be intrinsic AGB stars as well. Since these are strong S stars, the C/O ratio in modeling the stars was set to 1 (Zook 1985) or to 0.98 (Lambert et al. 1995). The isotopic composition of Zr in the stars was determined from the intensities of isotopically shifted lines in spectra of the ZrO molecule. The uncertainties in the astronomical observations are difficult to determine and they were evaluated for three of the data points of Lambert et al. (1995). These uncertainties are plotted in Figure 3 and the relative uncertainties of the other data points are expected to be similar. The initial $^{93}$Zr/Zr fractions in the grains, which were the same as in the envelopes of the grains' source stars, are taken as the present-day Nb/(Zr+Nb) ratio in the grains. Due to the Zr depletion in the grains (Section 3.2 and Figure 2) and the unknown initial (nonradiogenic) Nb content of the grains, the Nb/(Zr+Nb) ratios in the grains are higher than the initial $^{93}$Zr/Zr fractions in them. However, the comparison could still be informative. The situation is similar to Figure 1, where despite the displacement of the grain data points relative to the radiogenic array, the fact that they plot close to it is important for interpreting the data. Also plotted in Figure 3 (at the bottom of the plot) is the range of *s*-process calculation results for the $^{93}$Zr/Zr ratio in a 2 $M_{\odot}$ solar metallicity AGB star.

The comparison in Figure 3 shows that the presolar grain data plot as expected above the calculated range of *s*-process composition (the composition of nine of the 19 grains agree within uncertainties with the *s*-process calculations) and that the astronomical observations agree (within uncertainties) with the *s*-process calculations. Interestingly, despite the Zr depletion in the grains, the compositions of the two data sets agree with one another for the most part (within uncertainties). This agreement suggests that the grains came from similar types of stars to the S stars that were observed. However, any attempt to reach firm conclusions regarding the relationship between $^{93}$Zr in the grains and in the astronomical data is currently impaired by the small number of astronomical observations available, and the large uncertainties in the astronomical data and in some of the grain data.

### 3.4. The $^{93}Zr(n,\gamma)^{94}Zr$ Cross Section

The radiative neutron capture cross sections, $\sigma_{(n,\gamma)}$, of all the stable Zr isotopes and $^{93}$Zr have been remeasured in recent years at *s*-process energies at n_TOF (the European facility for neutron nuclear astrophysics at CERN; Mengoni 2002). While results have been published for the stable Zr isotopes (Tagliente et al. 2006, 2008a, 2008b), the new results for $^{93}$Zr have not been published yet. Our data do not suggest a correction to the recommended value, $\sigma^{93}_{(n,\gamma)} = 95 \pm 10$ mb ($1\sigma$ uncertainty) at 30 keV (Macklin 1985; Bao et al. 2000). However, cross section values ranging from 18% smaller than the recommended value to 11% larger are compatible with our interpretation of the data, suggesting that a potential correction would not be outside this range. This range is narrower than the $2\sigma$ uncertainty of the recommended value, ±21%.

## 4. SUMMARY

SXRF was applied to the analysis of trace elements in presolar grains for the first time in this study. Forty-one SiC grains of the KJF size-separate (mass-weighted median size of 1.86 $\mu$m) from the Murchison meteorite (CM2) were analyzed. The absolute abundances of Zr and Nb were measured simultaneously in 19 of the grains. Since the isotopic compositions of the grains were not measured, the grains were assumed to be mainstream grains (that make up 93% of all presolar SiC grains).

When comparing the grain data with *s*-process model calculations for low mass AGB stars on a plot of Nb abundance versus Zr abundance, the grains plot close to the array of results which include the radiogenic contribution to Nb from $^{93}$Zr. This indicates that the relatively short-lived *s*-isotope $^{93}$Zr ($t_{1/2} = 1.5 \times 10^6$ yr) condensed into the grains and decayed *in situ* to $^{93}$Nb (the only stable isotope of Nb).

The displacement of 15 of the 19 grain data points relative to the *s*-process $^{93}$Zr radiogenic array, coupled with low Zr enrichment factors in some grains, indicates that the grains are depleted in Zr to varying degrees. This suggests that the grains condensed from stellar atmospheres that were depleted in Zr, but not in Nb. Zirconium is more abundant in AGB stars and a little more refractory than Nb. Hence, Zr could have been depleted from the stellar gas by early condensation of ZrC and removal by radiation pressure. In addition, ZrC could have been captured in grains of, or formed solid solution with, the more abundant phases TiC and graphite. The high Nb/Zr in the 15 grains could be due as well to a combination of Zr depletion and contamination with solar system Nb, in the Murchison meteorite or in the laboratory.

The Nb/Zr ratios in the grains were taken as upper limits on the initial $^{93}$Zr/Zr ratios in the grains and compared with the $^{93}$Zr/Zr ratios in nine late-type S stars, the only stars for which the ratio was measured. Both data sets agree within uncertainties. As expected, while the astronomical data agree with the range of *s*-process calculation results, half of the grains plot above it.

The neutron capture cross section of $^{93}$Zr at *s*-process energies was remeasured in recent years (results are yet to be published). While our data do not suggest a correction to the recommended value, $\sigma^{93}_{(n,\gamma)} = 95 \pm 10$ mb at 30 keV ($1\sigma$ uncertainty), values ranging from 18% smaller to 11% larger are compatible with our interpretation of the data. This range is narrower than the $2\sigma$ uncertainty of the recommended value, ±21%.

In the future, it would be highly desirable to expand the application of synchrotron X-ray techniques to the study of trace elements in presolar grains and combine them with other experimental techniques. One example is the application SXRF to the analysis of trace elements in other, and less studied, types of presolar grains, like graphite and silicates. Another example is to develop a method to combine analysis of the same single presolar grains by SXRF and other synchrotron X-ray techniques, like XANES and EXAFS, which give different chemical information, like the trace element local chemical environment (which could potentially be used to infer the chemical form of trace elements in the host grain), with isotopic analysis techniques, like SIMS and RIMS. This would further our understanding of the nucleosynthesis and chemistry that determined the compositions of the grains.

We thank Sachiko Amari and Roy S. Lewis for sharing their Murchison KJF sample. Helpful discussions with Roy S. Lewis and Michael Paul are greatly appreciated. We thank Thomas J. Bernatowicz and Thomas K. Croat for helpful discussions and for sharing unpublished data. Reviews by Katharina Lodders and two anonymous reviewers greatly improved the paper. This work was supported by the National Aeronautics and Space Administration through grants to A.M.D. and R.N.C. R.G. acknowledges support by the Italian MIUR-FIRB project "Astrophysical origin of elements beyond the Fe peak." Use of the Advanced Photon Source was supported by the U.S. Department of Energy, Office of Science, Office of Basic Energy Sciences, under Contract No. W-31-109-ENG-38.

## REFERENCES

Amari, S., Gao, X., Nittler, L. R., Zinner, E., Jose, J., & Hernanz, M. 2001a, ApJ, 551, 1065
Amari, S., Hoppe, P., Zinner, E., & Lewis, R. S. 1995, Meteoritics, 30, 679
Amari, S., Lewis, R. S., & Anders, E. 1994, Geochim. Cosmochim. Acta, 58, 459
Amari, S., Nittler, L. R., Zinner, E., Lodders, K., & Lewis, R. S. 2001b, ApJ, 559, 463
Anders, E., & Grevesse, N. 1989, Geochim. Cosmochim. Acta, 53, 197
Anders, E., & Zinner, E. 1993, Meteoritics, 28, 490
Bao, Z. Y., Beer, H., Käppeler, F., Voss, F., Wisshak, K., & Rauscher, T. 2000, At. Data Nucl. Data Tables, 76, 70
Barzyk, J. G., Savina, M. R., Davis, A. M., Gallino, R., Pellin, M. J., Lewis, R. S., Amari, S., & Clayton, R. N. 2006, New Astron. Rev., 50, 587
Barzyk, J. G., et al. 2008, Lunar Planet. Sci. XXXIX, 1986 (abstract)
Bernatowicz, T. J., Akande, O. W., Croat, T. K., & Cowsik, R. 2005, ApJ, 631, 988
Bernatowicz, T. J., Cowsik, R., Gibbons, P. C., Lodders, K., Fegley, B., Jr., Amar, S., & Lewis, R. S. 1996, ApJ, 472, 760
Bruland, K. W., & Lohan, M. C. 2003, in Treatise on Geochemistry, Vol. 6, The Oceans and Marine Geochemistry, ed. H. Elderfield, H. D. Holland, & K. K. Turekian (Oxford: Elsevier), 23
Busso, M., Gallino, R., & Wasserburg, G. J. 1999, ARA&A, 37, 239
Clayton, D. D., & Nittler, L. R. 2004, ARA&A, 42, 39
Croat, T. K., Stadermann, F. J., & Bernatowicz, T. J. 2005, ApJ, 631, 976
Gallino, R., Arlandini, C., Busso, M., Lugaro, M., Travaglio, C., Straniero, O., Chieffi, A., & Limongi, M. 1998, ApJ, 497, 388
Hoppe, P., Amari, S., Zinner, E., Ireland, T., & Lewis, R. S. 1994, ApJ, 430, 870
Hoppe, P., Annen, P., Strebel, R., Eberhardt, P., Gallino, R., Lugaro, M., Amari, S., & Lewis, R. S. 1997, ApJ, 487, L101
Jochum, K. P., Stolz, A. J., & McOrist, G. 2000, Meteorit. Planet. Sci., 35, 229
Kashiv, Y. 2004, PhD Thesis, Univ. Chicago
Kashiv, Y., Cai, Z., Lai, B., Sutton, S. R., Lewis, R. S., Davis, A. M., Clayton, R. N., & Pellin, M. J. 2001, Lunar Planet. Sci. XXXII, 2192 (abstract)
Kashiv, Y., Cai, Z., Lai, B., Sutton, S. R., Lewis, R. S., Davis, A. M., Clayton, R. N., & Pellin, M. J. 2002, Lunar Planet. Sci. XXXIII, 2056 (abstract)

Kashiv, Y., Davis, A. M., Cai, Z., Lai, B., Sutton, S. R., Lewis, R. S., Gallino, R., & Clayton, R. N. 2006, Lunar Planet. Sci. XXXVII, 2464 (abstract)
Knight, K. B., et al. 2008, Lunar Planet. Sci. XXXIX, 2135 (abstract)
Lambert, D. L., Smith, V. V., Busso, M., Gallino, R., & Straniero, O. 1995, ApJ, 450, 302
Lodders, K., & Fegley, B., Jr. 1995, Meteoritics, 30, 661
Lodders, K., & Fegley, B., Jr. 1997, ApJ, 484, L71
Lodders, K., Palme, H., & Gail, H.-P. 2009, in Landolt-Börnstein, New Series, Vol. VI/4B, ed. J. E. Trümper (Berlin: Springer), 560 (arXiv:0901.1149)
Lugaro, M., Davis, A. M., Gallino, R., Pellin, M. J., Straniero, O., & Käppeler, F. 2003, ApJ, 593, 468
Macklin, R. 1985, Ap&SS, 115, 71
McKeegan, K. D., et al. 2006, Science, 314, 1724
Mengoni, A. 2002, in Astrophysics, Symmetries, and Applied Physics at Spallation Neutron Sources, ed. P. E. Koehler et al. (Singapore: World Scientific), 25
Messenger, S., Keller, L. P., Stadermann, F. J., Walker, R. M., & Zinner, E. 2003, Science, 300, 105
Münker, C., Pfänder, J. A., Weyer, S., Büchl, A., Kleine, T., & Mezger, K. 2003, Science, 301, 84
Nguyen, A. N., Busemann, H., & Nittler, L. R. 2007, Lunar Planet. Sci. XXXVIII, 2332 (abstract)
Nittler, L. R., & Alexander, M. O'D. 2003, Geochim. Cosmochim. Acta, 67, 4961
Peery, B. F., & Beebe, R. F. 1970, ApJ, 160, 619
Savina, M. R., Davis, A. M., Tripa, C. E., Pellin, M. J., Gallino, R., Lewis, R. S., & Amari, S. 2004, Science, 303, 649
Sharp, C. M., & Wasserburg, G. J. 1995, Geochim. Cosmochim. Acta, 59, 1633
Smith, V. V., & Lambert, D. L. 1990, ApJS, 72, 387
Tagliente, G., et al. 2006, in Nuclei in the Cosmos-IX, Proceedings of Science, SISSA, Trieste, 2006, ed. A. Mengoni et al., http://pos.sissa.it//archive/conferences/028/227/NIC IX_227.pdf
Tagliente, G., et al. 2008a, Phys. Rev. C, 77, 035802
Tagliente, G., et al. 2008b, Phys. Rev. C, 78, 045804
Travaglio, C., Gallino, R., Arnone, E., Cowan, J., Jordan, F., & Sneden, C. 2004, ApJ, 601, 864
Weyer, S., Munker, C., Rehkamper, M., & Mezger, K. 2002, Chem. Geol., 187, 295
Yada, T., et al. 2005, Lunar Planet. Sci. XXXVI, 1227 (abstract)
Zinner, E. 1998, Annu. Rev. Earth Planet. Sci., 26, 147
Zinner, E., Nittler, L. R., Gallino, R., Karakas, A. I., Lugaro, M., Straniero, & Lattanzio, J. C. 2006, ApJ, 650, 350
Zook, A. C. 1985, ApJ, 289, 356